STEM CELLS TRANSLATIONAL MEDICINE®

TISSUE-SPECIFIC PROGENITOR AND STEM CELLS

Safety of Human Neural Stem Cell Transplantation in Chronic Spinal Cord Injury

KATJA M. PILTTI,[a,b,c,d,*] DESIREE L. SALAZAR,[a,d,e,*] NOBUKO UCHIDA,[f] BRIAN J. CUMMINGS,[a,b,c,d] AILEEN J. ANDERSON[a,b,c,d]

Key Words. Spinal cord injury • Neural stem cell • Chronic transplantation • Fate • Migration • CGRP • Mechanical allodynia • Thermal hyperalgesia

[a]Sue and Bill Gross Stem Cell Research Center, [b]Physical and Medical Rehabilitation, [c]Institute for Memory Impairments and Neurological Disorders, and [d]Anatomy and Neurobiology, University of California Irvine, Irvine, California, USA; [e]Ludwig Institute for Cancer Research, University of California San Diego, La Jolla, California, USA; [f]StemCells Inc., Newark, California, USA

[*]Contributed equally as first authors.

Correspondence: Aileen J. Anderson, Ph.D., 2030 Gross Hall Stem Cell Center, University of California Irvine, Irvine, California 92697, USA. Telephone: 949-824-6750; Fax: 949-824-9728; E-Mail: aja@uci.edu

Received April 2, 2013; accepted for publication July 10, 2013; first published online in SCTM *EXPRESS* November 4, 2013.

1066-5099/2013/$20.00/0

http://dx.doi.org/10.5966/sctm.2013-0064

ABSTRACT

The spinal cord injury (SCI) microenvironment undergoes dynamic changes over time, which could potentially affect survival or differentiation of cells in early versus delayed transplantation study designs. Accordingly, assessment of safety parameters, including cell survival, migration, fate, sensory fiber sprouting, and behavioral measures of pain sensitivity in animals receiving transplants during the chronic postinjury period is required for establishing a potential therapeutic window. The goal of the study was assessment of safety parameters for delayed transplantation of human central nervous system-derived neural stem cells (hCNS-SCns) by comparing hCNS-SCns transplantation in the subacute period, 9 days postinjury (DPI), versus the chronic period, 60 DPI, in contusion-injured athymic nude rats. Although the number of surviving human cells after chronic transplantation was lower, no changes in cell migration were detected between the 9 and 60 DPI cohorts; however, the data suggest chronic transplantation may have enhanced the generation of mature oligodendrocytes. The timing of transplantation did not induce changes in allodynia or hyperalgesia measures. Together, these data support the safety of hCNS-SCns transplantation in the chronic period post-SCI. STEM CELLS TRANSLATIONAL MEDICINE *2013;2:961–974*

INTRODUCTION

Worldwide, an estimated 5.3 million people are living with a chronic spinal cord injury (SCI), which yields an estimated global incidence of 380,000 new injuries per year (reviewed in [1, 2]). In parallel, an estimated 1.3 million individuals are living with chronic SCI in the U.S., which yields an estimated incidence of 20,000 new injuries annually (reviewed in [3]; see also http://www.christopherreeve.org and http://www.cdc.gov). In the past four decades, the mortality rate during the first year of SCI has been successfully reduced [3]; however, no effective therapy has been developed so far.

Preclinical data collected during the past decade suggest that neural stem cell transplantation may have the potential to yield repair and recovery of function in central nervous system (CNS) injury and disease, including SCI. In our previous studies, we have shown that human central nervous system-derived stem cells propagated as neurospheres (hCNS-SCns) exhibit robust engraftment and improved locomotor recovery when transplanted 9 or 30 days post-SCI into the spared parenchyma rostral and caudal to the injury epicenter in rodent models [4–6]. In injured spinal cords, hCNS-SCns differentiated into all three neural lineages; however, a majority of the cells adopted an oligodendrocyte fate [4–6]. hCNS-SCns-origin cells remyelinated host axons and formed synapses with host neuronal circuitry but did not alter regeneration, lesion volume, lesion scar, or angiogenesis [5], suggesting cell integration as a mechanism for recovery of function. Recently, we compared hCNS-SCns transplantation into the injury epicenter versus intact rostral/caudal spinal cord parenchyma in contusion-injured athymic nude (ATN) rats [7]. The data suggested that in ATN rats, which form a cystic cavity after SCI similar to that found in a majority of human clinical injuries, the intact rostral/caudal parenchyma may be a more favorable transplantation site than the injury epicenter at subacute period postinjury [7]. The total number of hCNS-SCns in animals receiving rostral/caudal parenchyma transplants was twice that of animals receiving epicenter transplants; furthermore, epicenter transplantation shifted the localization of cells entering the astroglial lineage. Additionally, total human cell engraftment and astroglial fate after epicenter transplantation were correlated with calcitonin gene-related peptide (CGRP) fiber sprouting, although no changes in mechanical allodynia or thermal hyperalgesia were observed [7].

The vast majority of studies evaluating cell transplantation in SCI animal models have focused on subacute grafting, administering cells

between 7 and 10 days postinjury (DPI) (reviewed in [8]). Despite the intense research focus on cell transplantation subacutely after SCI, the chronic stage of injury is an appealing potential time point to initiate cell therapy for several reasons. Among these, 75% of American Spinal Injury Association/International Spinal Cord Society (ASIA/ISCoS) neurological standard scale (AIS) conversions are estimated to occur within 3 months post-SCI, and therefore delayed administration of a therapeutic agent or cells in clinical trial testing may yield more reliable safety/efficacy data and lower the number of subjects required to achieved adequate statistical power [9]. Delayed treatment may also permit better informed consent and improved tolerability for the side effects related to immunosuppressive drugs [10].

Although a precise definition of the chronic postinjury phase in humans and animal models has not been established, the operational definition is built around stabilization of spontaneous recovery of function. In humans, this translates to approximately 6–12 months postinjury [9, 11, 12]; in rodent models, this translates to 1–2 months postinjury [11, 13, 14]. Critically, the microenvironment within the injured spinal cord changes over time and with location relative to the epicenter [11, 15–20], potentially altering donor cell survival, proliferation and differentiation in the host tissue [7, 21, 22, 23] (Hooshmand MJ, Nguyen HX, Hong S et al., submitted for publication), and necessitating assessment of safety and efficacy at multiple time points post-SCI and based on the site of delivery to establish a potential therapeutic window.

Cell transplantation in chronic SCI models at 2 months or longer postinjury has been previously evaluated using different cell types including nonhuman Schwann cells, olfactory ensheathing glia, bone-marrow stromal cells, and neural stem cells/progenitors, and human oligodendrocyte progenitors (reviewed in [8, 24]). Only a few of these studies reported some level of functional recovery, and so far, there is no solid preclinical evidence supporting either the safety or efficacy of stem cell transplantation in chronic SCI (reviewed in [8]). Accordingly, in this study, we investigated the safety of hCNS-SCns in the chronic SCI microenvironment in the ATN rat, comparing parenchymal transplantation at either 9 or 60 DPI. We assessed human cell engraftment, survival, migration, fate, and development of anatomical or behavioral evidence of neurological pain (allodynia and hyperalgesia) using von Frey, Hargreaves, and CatWalk measures [25–29]. Overall, the data suggest that hCNS-SCns engraft, migrate, and differentiate in the chronic SCI environment without adverse effects.

Materials and Methods

Animal Welfare

This study was carried out in accordance with the Institutional Animal Care and Use Committee at the University of California, Irvine, and in consistency with U.S. Federal guidelines.

Contusion Injuries and hCNS-SCns Transplantation

ATN rats, 180–200 g, (National Cancer Institute, Frederick, MD, http://ncifrederick.cancer.gov) were anesthetized and T9 vertebrae were laminectomized prior administration of incomplete bilateral, moderate 200-kD contusion injuries as described [7]. Following the injury, even bilateral bruising was confirmed under a microscope, the exposed spinal cords were covered, muscles and skin were sutured, and postoperative care was performed as described previously [7]. Animals in the 9 DPI and 60 DPI cohorts received spinal cord injuries at the same postnatal age (10–11 weeks) during two sequential weeks of surgery, that is, 9 DPI and 60 DPI cohort animals were injured 1 week apart. Data presented therefore reflect a direct comparison across cohorts and do not use historical data.

hCNS-SCns (StemCells Inc., Palo Alto, CA, http://www.stemcellsinc.com) were cultured as neurospheres in supplemented X-Vivo 15 medium (Lonza, Basel, Switzerland, http://www.lonza.com) as previously described [30]. Prior to transplantation, neurospheres at passage number 12 or less were dissociated into individual cells and adjusted into a cell density of 50,000 cells per microliter in X-Vivo 15 medium (Lonza). Rats were reanesthetized either 9 or 60 DPI, the laminectomy sites re-exposed, and the cords stabilized in a spinal stereotaxic frame. A total volume of 4 μl (1 μl per injection site) of cell suspension or vehicle (X-Vivo 15 medium) was injected in two rostral bilateral injections through the intervertebral cartilage space at T7/T8 and another two caudal injections through the intervertebral cartilage space at T10/T11 using polished 30° beveled glass pipettes, inner diameter = 75–80 μm, outer diameter = 100–115 μm (Sutter Instruments, Novato, CA, http://www.sutter.com), a NanoInjector 2000 system (World Precision Instruments, Waltham, MA, http://www.wpiinc.com), and a micropositioner (World Precision Instruments) under microscopic guidance. After transplantation, the postoperative procedures were performed as described in [7].

Randomization, Exclusion Criteria, and Group *n* Values

Randomization, exclusion criteria, and blinding for assessments were conducted as described previously [4–7]. Prior to transplantation, rats ($n = 71$) were randomized across cohorts, and equivalent behavioral baselines were confirmed for each cohort using pretransplant Basso, Beattie, and Bresnahan (BBB) locomotor scores 7 or 55 DPI (see also Behavioral Assessments). Animals with abnormal scores (>2 SDs outside the cohort mean), unilateral bruising, or abnormal force/displacement curves after contusion injury, or in which a vertebral T9 laminectomy could not be confirmed at the time of cell transplantation, were excluded from the study. An additional eight animals were lost because of anesthesia/surgery-related complications. After these exclusions behavioral and histological assessments were completed in $n = 47$ animals. All animal care, behavioral assessments, and histological processing/analysis were performed by observers blinded to the experimental cohorts.

hCNS-SCns engraftment was confirmed in all animals, and a subset of spinal cords from animals in all cohorts was randomly selected for stereological analysis. SC121 immunostaining revealed that 2 of 9 rats from the 9 DPI hCNS-SCns cohort and 4 of 11 rats from the 60 DPI hCNS-SCns cohort showed very poor or no engraftment; these rats were excluded from further sensory behavioral and stereological analysis, and from statistical analysis other than reporting of the percentage of engrafted animals. Final cohort numbers (n) for sensory assessment were therefore as follows: 9 DPI hCNS-SCns, $n = 10$; 9 DPI vehicle, $n = 12$; 60 DPI hCNS-SCns, $n = 7$; 60 DPI vehicle, $n = 12$. Final cohort numbers for histology/stereology or evaluation of locomotor function at 14 weeks post-transplantation (WPT) were as follows: 9 DPI hCNS-SCns, $n = 7$; 9 DPI vehicle, $n = 8$; 60 DPI hCNS-SCns, $n = 7$; 60 DPI vehicle, $n = 12$ (supplemental online Table 1).

Behavioral Assessments

Mechanical allodynia assessment using von Frey testing [26] and thermal hyperalgesia assessment using Hargreaves testing [25] were conducted prior to injury (baseline), and at 2, 7, 11, and 14 WPT as described in [7]. CatWalk video of three individual runs per animal was recorded at 14 WPT and analyzed using CatWalk software version 6.13 for Windows by individuals blinded to experimental groups [7]. Hind limb base of support measures are shown relative to baseline obtained in uninjured ATN rats assessed at 7 weeks of age.

BBB open-field testing was performed as published by Basso et al. [13]; however, we found assessment of coordination on the BBB in the ATN rat strain to be flawed. Specifically, the number of "passes" in which locomotion was carried out at a consistent speed for an assessable distance was too low to achieve an acceptable degree of accuracy, regardless of the amount of habituation to the task the animals received or manipulation of task parameters. Pretransplantation BBB scores were not critically affected because they ranged below the affected portion of the BBB scale, particularly in the case of the 9 DPI cohort. However, by several weeks post-transplant, a majority of the animals were performing within the range of the BBB rating scale where accurate assessment of coordination was critical. To address this issue, we used the 14 WPT CatWalk data to establish a coordination score for the 14 WPT BBB data, as previously described by Hamers et al. [31]. Using this method, the achievement of a score for regularity index (RI) = 100% in three of three CatWalk runs was awarded a BBB rating score of consistent coordination. RI = 100% in two of three CatWalk runs was awarded a BBB rating score of frequent coordination. RI = 100% in one of three CatWalk runs was awarded a BBB rating score of occasional coordination. RI = 100% in 0 of 3 CatWalk runs was awarded a BBB rating score of no coordination. Accordingly, only pretransplant BBB data and 14 WPT BBB data are included herein.

Perfusion, Tissue Collection, Sectioning, and Immunohistochemistry

At 14 WPT, rats were terminally anesthetized and transcardially perfused, T6–T12 vertebral regions were dissected based on dorsal spinal root counts, postfixed, flash frozen, and stored for sectioning as described in [7]. Whole T6–T12 spinal cord segments were cut into 30-μm-thick coronal sections using MultiCord technology (NeuroScience Associates, Knoxville, TN, http://www.neuroscienceassociates.com) or a cryostat (Thermo Fisher Scientific, Waltham, MA, http://www.thermofisher.com) followed by mounting onto slides using a CryoJane tape transfer system (Leica Biosystems, Inc., Buffalo Grove, IL, http://leicabiosystems.com). For 3,3′-diaminobenzidine immunohistochemistry, the tissue sections were antigen-retrieved and treated to deactivate endogenous peroxide activity, and immunostained as described in [5, 7]. Hematoxylin, or methyl green counterstain was used to visualize nuclei (Sigma-Aldrich, St. Louis, MO, http://www.sigmaaldrich.com). Fluorescence-conjugated immunohistochemistry was performed as described in [5, 7].

The primary antibodies used were directed against human cytoplasm SC121 (STEM121; StemCells Inc., Newark, CA, http://www.stemcellsinc.com); human glial fibrillary acidic protein (GFAP) SC123 (STEM123; StemCells Inc.); pan-GFAP (BD Pharmingen, San Diego, http://www.bdbiosciences.com), doublecortin (DCX) (Santa Cruz Biotechnology Inc., Santa Cruz, CA, http://www.scbt.com), β-tubulin III (βTub III) (Covance, San Diego, CA, http://www.covance.com), Olig2 (R&D Systems Inc., Minneapolis, MN, http://www.rndsystems.com), APC (EMD Millipore, Darmstadt, Germany, http://www.millipore.com), and CGRP (Sigma-Aldrich). The secondary antibodies used were DyLight fluorescence-conjugated affinipure F(ab′)$_2$ fragment secondary antibodies (Jackson Immunoresearch Laboratories, West Grove, PA, http://www.jacksonimmuno.com) or Alexa Fluor 555 or 488 IgG subclass-specific secondary antibodies (Invitrogen, Carlsbad, CA, http://www.invitrogen.com). Hoechst 33342 (Invitrogen) was used for nuclear labeling. The *z*-stacks of optical sections were acquired using an ApoTome system on a Zeiss AxioImager M2 microscope (Carl Zeiss, Maple Grove, MN, http://www.zeiss.com).

Stereological Quantification

Final animal numbers for analysis are as described above and listed in supplemental online Table 1. Total numbers of SC121$^+$ human cells were determined by unbiased stereology in 1 of 24 intervals from spinal cord sections 0.72 mm apart using systematic random sampling with an optical fractionator probe and StereoInvestigator version 9 (MicroBrightField Inc., Williston, VT, http://www.mbfbioscience.com). Optical fractionator grid size and counting frame size were empirically determined to yield average Gundersen cumulative error values less than 0.1 (supplemental online Table 2). The numbers of SC123$^+$, SC121$^+$/Olig2$^+$, SC121$^+$/DCX$^+$, SC121$^+$/APC$^+$(CC-1)/Olig2$^+$, and SC121$^+$/APC$^+$(CC-1)/Olig2$^-$ cells were analyzed in 1 of 48 intervals from spinal cord sections 1.44 mm apart using an optical fractionator probe and systematic random sampling according to stereological principles (supplemental online Table 2).

A Cavalieri probe (SI9; MicroBrightField) was used to analyze total volumes of spinal cord, lesion, and dorsal horn CGRP fibers in 1 of 24 intervals from coronal spinal cord sections 0.72 mm apart at $\times$4 magnification (supplemental online Table 2). A spaceball probe with a 12-μm hemisphere was used to analyze CGRP fiber length in dorsal horn lamina III and IV rostral to lesion cavity in 1 of 24 intervals from coronal spinal cord sections 0.72 mm apart. A contour was drawn around laminae III and IV at $\times$60 magnification, identified by the pattern of nuclear staining, and the fiber length was assessed at $\times$100 magnification (supplemental online Table 2).

The migration of human cells was analyzed as percentage of the cells per section relative to total number of counted SC121$^+$ human cells. The distribution of the cells was normalized with the distance from the injury epicenter, designated as the most damaged tissue section with largest cavity.

Statistical Analysis

All data are shown as mean $\pm$ SEM; statistical analysis was performed using Prism software, version 4 (GraphPad Software, Inc., San Diego, CA, http://www.graphpad.com). von Frey and Hargreaves scores were compared using two-way repeated-measures analysis of variance (ANOVA) combined with Bonferroni post hoc *t* tests. Correlation between CGRP length or volume, numbers of SC123$^+$ or SC121$^+$ cells, and Hargreaves or von Frey measures was assessed using the Pearson correlation coefficient. Comparisons between the cohorts were analyzed using either one-way ANOVA combined with Tukey's post hoc *t* test or Student's two-tailed *t* test. A p value $\leq$.05 was considered to be statistically significant.

RESULTS

hCNS-SCns Transplanted in Chronic Rat Contusion SCI Survive, Engraft, Migrate, and Do Not Alter Lesion or Spared Tissue Volume

To determine hCNS-SCns engraftment in the transplanted spinal cords at 14 WPT, we performed immunohistochemistry using a human cytoplasm-specific antibody, SC121. As expected, neither the 9 or 60 DPI vehicle cohorts exhibited positive staining for SC121 at 14 WPT (Fig. 1A). Cohort animal numbers for analysis were as described in Materials and Methods and in supplemental online Table 1. Animals that exhibited either caudal/rostral-only engraftment (presumed to be injection failure) or no detectable human cells were excluded from further analysis (as described in Materials and Methods and indicated in red in Fig. 1C). In the 9 DPI hCNS-SCns transplantation cohort, $SC121^+$ human cells were found in seven of nine spinal cords at 14 WPT (88.9% engraftment; Fig. 1B, 1C). Unbiased stereological quantification estimates revealed an average of 1,114,000 $\pm$ 94,780 $SC121^+$ human cells (557 $\pm$ 47% of the initial transplant dose) in the spinal cords of 9 DPI hCNS-SCns cohort animals at 14 WPT (data previously published in [7]; Fig. 1C). In comparison, in the 60 DPI hCNS-SCns cohort, $SC121^+$ human cells were found in 7 of 11 spinal cords at 14 WPT (63.6% engraftment; Fig. 1C). Unbiased stereological quantification estimates revealed an average of 550,400 $\pm$ 153,600 $SC121^+$ human cells (275 $\pm$ 77% of the initial transplant dose) in the spinal cords of 60 DPI hCNS-SCns cohort animals at 14 WPT (Fig. 1C). Engrafted animals in the 60 DPI compared with the 9 DPI hCNS-SCns transplantation cohort exhibited a significant decrease in human cell number as determined at 14 WPT (Student's two-tailed *t* test; **, $p < .009$). This suggests that although hCNS-SCns engraft in both the subacute and chronic injury environment, the microenvironmental cues promoting donor cell survival and/or proliferation may change over time after SCI. This detailed histological analysis showed no evidence of abnormal cellular morphology or mass formation in any of the cohorts.

Changing microenvironmental cues could potentially affect not just survival/proliferation but also migration. For example, rodent neural precursors have shown to exhibit different patterns of cell migration after transplantation in acute or chronic phase of CNS injury [11, 32]. For migration analysis, spinal cord sections were aligned by location relative to the injury epicenter, designated as the most damaged tissue section. In both the 9 and 60 DPI hCNS-SCns transplantation cohorts, the majority of $SC121^+$ human cells were localized in the intact parenchyma away from both the injection sites and the injury epicenter (Fig. 1D; supplemental online Movies 1 and 2). No significant differences in hCNS-SCns localization were observed between the 9 or 60 DPI transplantation cohorts (Fig. 1D, 1E; Student's two-tailed *t* test; $p > .05$), suggesting that the chronic SCI environment provided migration cues similar to those present in the subacute microenvironment.

Similarly to humans and other rat strains, the ATN rat forms a cystic cavity at the injury epicenter after SCI [33, 34]. The primary lesion cavity evolves over time after SCI. In the case of rat SCI, lesion volume initially expands after injury but starts to decrease after 7 DPI; by 14 DPI the lesion volume is reduced by half, and by 40 DPI it is decreased by threefold compared with the first week of injury [35]. We have not previously observed changes in lesion or spared spinal cord tissue volume after hCNS-SCns transplantation [5–7]. In accordance with these data, no significant differences in lesion or spared spinal cord tissue volumes were found between the 9 DPI transplant and 9 DPI vehicle control animals (data previously published; [7]), or the 60 DPI transplant and 60 DPI vehicle control animals (supplemental online Fig. 1; Student's two-tailed *t* test; $p > .05$), suggesting that timing of transplantation at the subacute or chronic stage of SCI did not affect lesion or spared tissue volume.

The Chronic SCI Microenvironment Promotes Trilineage hCNS-SCns Differentiation

To assess whether the chronic timing of the transplantation affects hCNS-SCns fate in immunodeficient ATN rats, we quantified the percentages of human cells positive for the human-specific astrocyte marker SC123 (human GFAP), the immature neuronal marker DCX, or the oligodendroglial lineage marker Olig2. Cytoplasmic Olig2 expression can reflect the generation of motor neurons in the developing spinal cord; however, nuclear Olig2 expression in the adult spinal cord is indicative of oligodendroglial differentiation. Accordingly, as previously reported, no overlap was detected between nuclear Olig2 staining and human origin $SC123^+$ astrocytes (supplemental online Fig. 2) or β-tubulin III^+ neurons (supplemental online Fig. 3).

Quantification of human origin $SC123^+$ astrocytes (Fig. 2A) revealed that the average proportion of human astrocytes in the 9 DPI hCNS-SCns cohort spinal cords was 41 $\pm$ 4.1%, and in 60 DPI hCNS-SCns cohort spinal cords was 34.3 $\pm$ 5.5%; no significant differences between these cohorts were found (Fig. 2B; Student's two-tailed *t* test; $p > .05$). In parallel, quantification of human DCX^+ neural lineage cells (Fig. 2C) revealed that the average proportion of $SC121^+/DCX^+$ cells in the 9 DPI hCNS-SCns cohort spinal cords was 6.1 $\pm$ 0.5%, and in the 60 DPI hCNS-SCns cohort spinal cords it was 9.8 $\pm$ 1.6%; again, no significant differences between the cohorts were found (Fig. 2D; Student's two-tailed *t* test; $p > .05$). As previously reported, a small proportion of human $SC121^+/DCX^+$ cells were also positive for the more mature neuronal marker β-tubulin III [7].

Finally, quantification revealed that the average proportion of $SC121^+/Olig2^+$ cells (Fig. 2E) in the 9 DPI hCNS-SCns cohort spinal cords was 52.0 $\pm$ 3.2%, and in the 60 DPI hCNS-SCns cohort spinal cords it was 38.4 $\pm$ 4.8%. This difference was statistically significant (Fig. 2F; Student's two-tailed *t* test; *, $p < .04$). Interestingly, although 99.1% of human cells in the 9 DPI cohort were positive for either GFAP, DCX, or Olig2, this combination of markers accounted for only 82.5% of human cells in the 60 DPI cohort (Fig. 3A). These data suggest that essentially all of cells in the 9 DPI cohort were lineage committed, whereas a significant fraction of human cells in the 60 DPI cohort were undetected by the differentiation markers used.

Although nuclear Olig2 expression is found in immature through fully differentiated oligodendrocytes, it is most consistent with early oligodendrocyte lineage cells [36, 37]. We therefore hypothesized that the unlabeled population of human cells in the 60 DPI hCNS-SCns cohort could be due to a change in cell lineage-specific maturation. Accordingly, we assessed the coexpression of nuclear Olig2 and the mature oligodendrocyte marker APC (CC-1) in the 60 DPI cohort. A small fraction (2.9 $\pm$ 1.4%) of $SC121^+$ human cells were positive for both nuclear Olig2 and CC-1 at 14 WPT (Fig. 3B–3E), supporting the progression of cells in the oligodendroglial lineage from nuclear Olig2 to

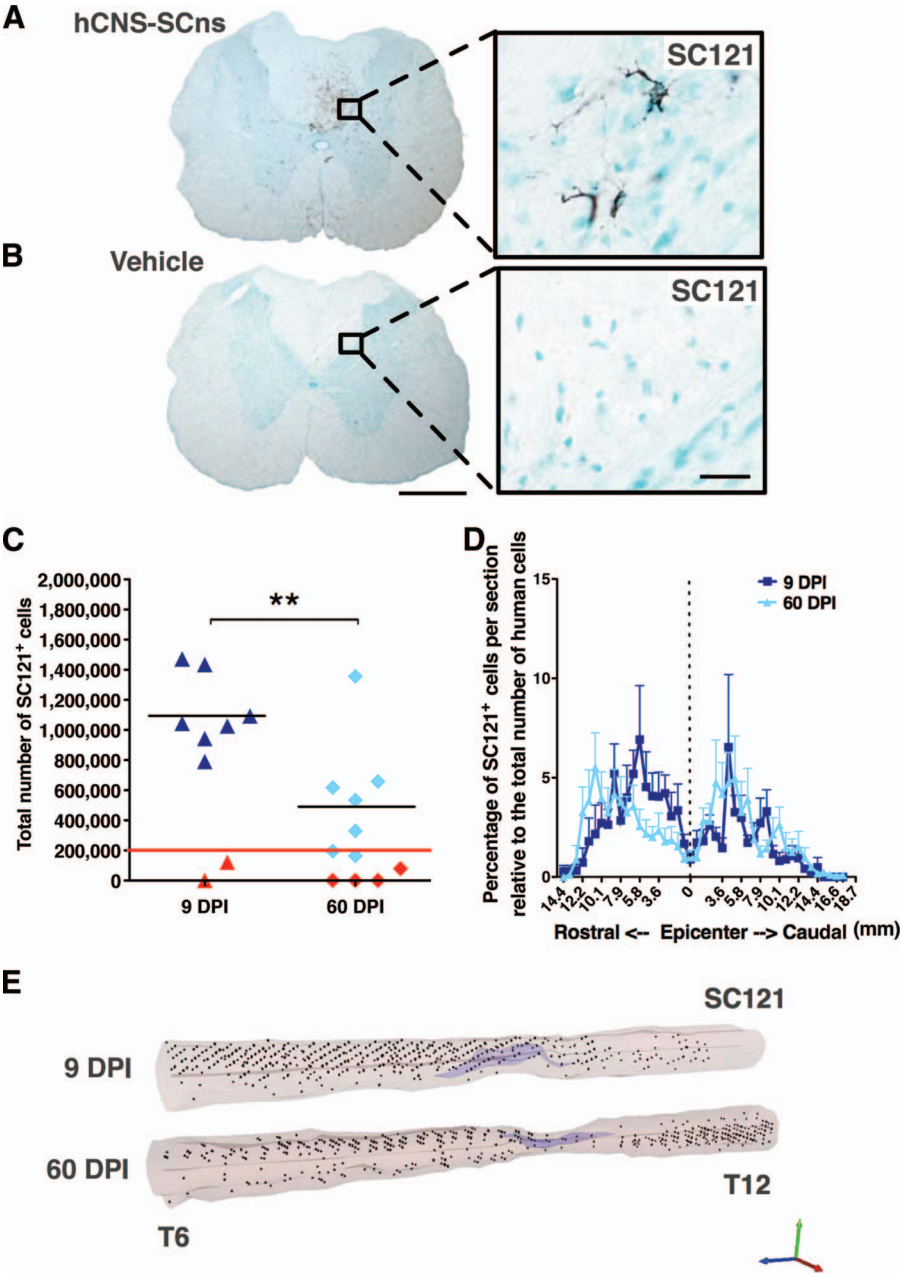

Figure 1. hCNS-SCns engraft, survive, and migrate when transplanted at either the subacute or chronic stage of spinal cord injury (SCI). Transplanted, engrafted spinal cords **(A)** showed human-specific cytoplasmic marker SC121$^+$ cells, unlike vehicle-treated cords **(B)** at 14 weeks post-transplantation (WPT). Scale bars = 500 μm (left) and 50 μm (right). Unbiased analysis using StereoInvestigator optical fractionator **(C)** revealed that the total estimated numbers of SC121$^+$ cells were significantly lower in the 60 DPI hCNS-SCns cohort compared with those in the 9 DPI hCNS-SCns cohort (Student's two-tailed *t* test; **, $p < .009$). Red line indicates the initial transplantation dose, black line indicates the average number of SC121$^+$ human cells, and red triangles indicate animals excluded because of poor engraftment. **(D):** Cell migration is shown as percentage of SC121$^+$ cells per section relative to total number of counted human cells (Student's two-tailed *t* test; $p > .05$). Positional data are plotted relative to the injury epicenter (vertical dashed line), which was designated based on identification of the tissue section containing the largest cross-sectional lesion area. Error bars shown as SEM. **(E):** Three-dimensional reconstruction of spinal cords transplanted at 9 or 60 DPI. The large cavities typical for athymic nude (ATN) rat SCI model are indicated in light purple, and the locations of analyzed SC121$^+$ human cells based on StereoInvestigator optical fractionator probe quantification data are represented by black dots. StereoInvestigator data were analyzed from coronal sections in a 1 of 24 sampling sequence at 14 WPT (StereoInvestigator data from the 9 DPI cohort in **[C]** were previously published in [7]). Abbreviations: DPI, days postinjury; hCNS-SCns, human central nervous system-derived neural stem cell.

CC-1 expression [37]. Quantification of triple labeling in the 60 DPI hCNS-SCns cohort revealed that 13.9 $\pm$ 2.4% of human cells were SC121$^+$/CC-1$^+$/Olig2$^-$ at 14 WPT (Fig. 3), supporting this hypothesis and suggesting that approximately 52.3% of human cells in the 60 DPI hCNS-SCns cohort differentiated into immature or mature oligodendrocyte lineage cells. The addition of quantification for terminally differentiated oligodendrocytes therefore raised the proportion of human cells exhibiting

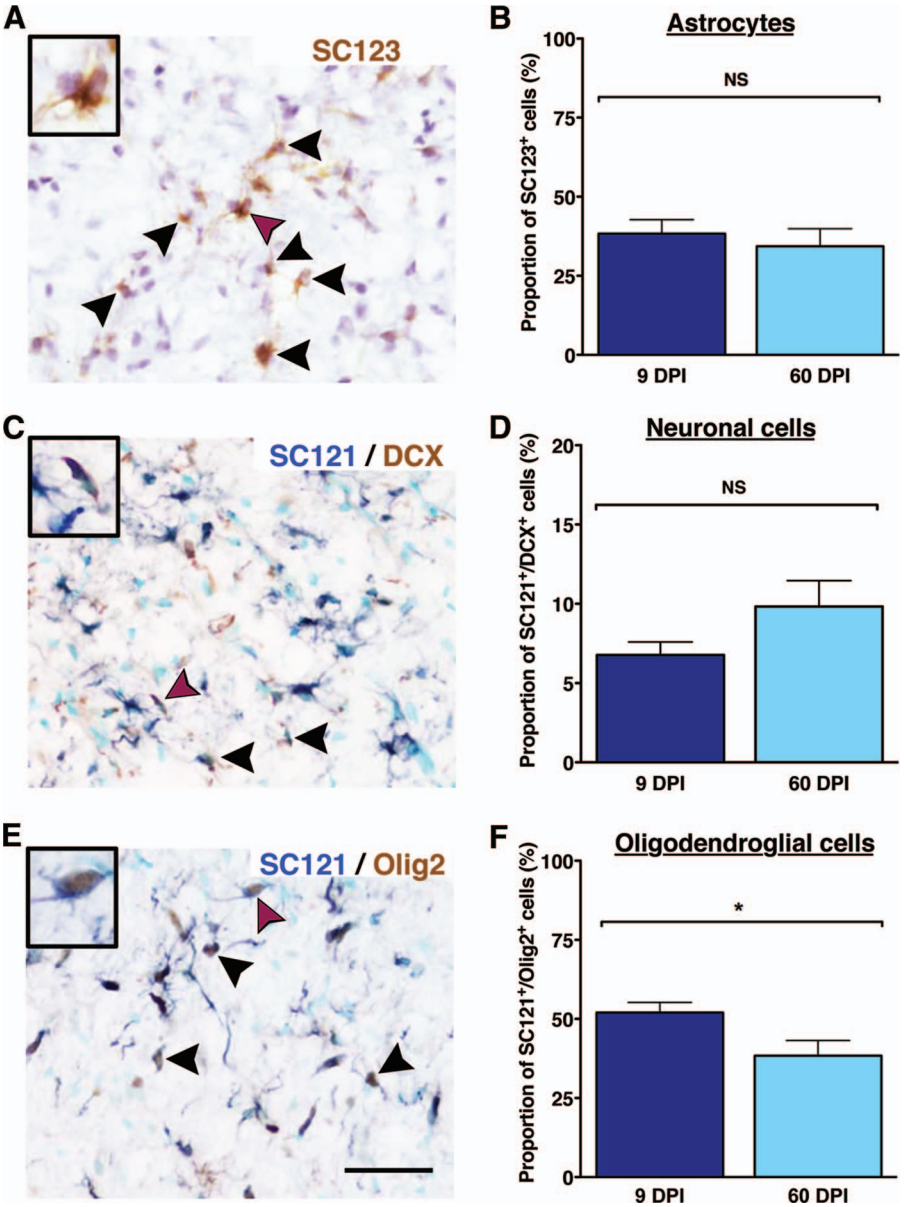

Figure 2. Human central nervous system-derived neural stem cell (hCNS-SCns) transplantation at 9 DPI versus 60 DPI does not affect differentiation into astroglial, neural, or oligodendroglial cell lineages at 14 weeks post-transplantation. The proportion of human-specific glial fibrillary acidic protein antibody SC123$^+$ cells (arrowheads) **(A)** did not differ between the 9 DPI and the 60 DPI transplant cohorts (Student's two-tailed *t* test; $*$, $p < .05$) **(B)**. Furthermore, the proportion of SC121$^+$/DCX$^+$ human immature neurons (arrowheads) **(C)** was not significantly different between the 9 DPI and the 60 DPI transplant cohorts (Student's two-tailed *t* test; $p > .05$) **(D)**. The majority of hCNS-SCns in both cohorts differentiated into SC121$^+$/Olig2$^+$ human oligodendroglial cells (arrowheads) **(E)**. However, the proportion of SC121$^+$/Olig2$^+$ cells was significantly decreased in the 60 DPI transplant cohort **(F)** compared with that in the 9 DPI transplant cohort (Student's two-tailed *t* test; $p < .05$). Cells marked with purple arrowheads are shown as insets. Scale bars = 50 μm. Error bars indicate SEM. Abbreviations: DCX, doublecortin; DPI, days postinjury; NS, not significant.

expression of lineage differentiation markers to 96.4%, equivalent to the fraction detected in the 9 DPI hCNS-SCns cohort (Fig. 3A). Taken together, this suggests that the chronic SCI microenvironment provides appropriate cues for hCNS-SCns differentiation and, surprisingly, that these cues may result in a more mature cellular phenotype for the oligodendroglial lineage.

hCNS-SCns Transplantation Does Not Alter CGRP Fiber Sprouting or Contribute to the Development of Allodynia or Hyperalgesia

Our previous studies have suggested that hCNS-SCns do not modulate the host spinal cord microenvironment by changing lesion or spared tissue volume [5, 7], NG2 deposition, GFAP astrogliosis, angiogenesis, or raphespinal descending serotoninergic or ascending CGRP fiber sprouting [5]. However, although these data suggest that hCNS-SCns transplantation does not alter host fiber sprouting, it is critical to assess this issue in multiple animal models. Chronic pain syndromes, such as allodynia (increased sensitivity to a stimulus that is not normally noxious) and hyperalgesia (enhanced sensitivity to a noxious stimulus), affect a high proportion of the SCI patient population and are related to the aberrant sprouting of ascending CGRP fibers into the deeper layers of the dorsal horn [38–41]. Induction of allodynia or hyperalgesia following stem cell transplantation would be a

A

hCNS-SCns-derived cell lineage	9 DPI	60 DPI
Total SC123 / DCX / Olig2	99 %	83 %
CC-1$^+$/Olig2$^-$	N/A	14 %
Total	**99 %**	**97 %**

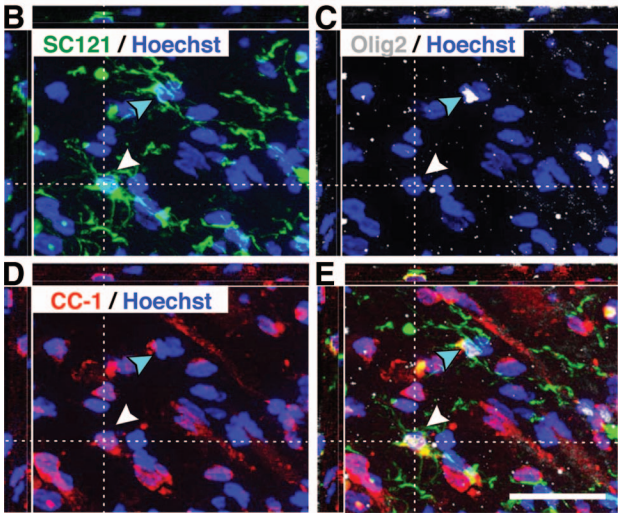

Figure 3. Lineage commitment of hCNS-SCns derived cells in athymic nude (ATN) rat spinal cord injury (SCI) model at 14 weeks post-transplantation (WPT). It was found that 99.1% of human cells in the 9 DPI cohort were positive for either glial fibrillary acidic protein, doublecortin, or Olig2 at 14 WPT, whereas this combination of markers accounted for only 82.5% of human cells in the 60 DPI cohort **(A)**. SC121/Olig2/APC (CC-1) triple immunostaining revealed that a significant fraction of human cells in the 60 DPI cohort were positive only for the mature oligodendroglial marker CC-1, and quantification of SC121$^+$/CC-1$^+$/Olig2$^-$ cells in the 60 DPI transplant cohort raised the proportion of human cells exhibiting expression of lineage differentiation markers to be equivalent to the fraction detected in the 9 DPI hCNS-SCns cohort **(A)**. **(B–E):** *xyz* projections show the 60 DPI cohort ATN rat spinal cord tissue at 14 WPT after immunohistochemistry using the human-specific cytoplasmic markers SC121 **(B)** and Olig2 **(C)** and the mature oligodendrocyte marker APC-1 (CC-1) **(D)** combined with nuclear counterstaining Hoechst. The overlay **(E)** demonstrates that some SC121$^+$ human cells expressed both nuclear Olig2 and CC-1 (turquoise arrowhead), whereas others were positive for the mature oligodendrocyte marker CC-1 only (white arrowhead). Scale bar = 25 μm. Abbreviations: DPI, days postinjury; hCNS-SCns, human central nervous system-derived neural stem cell; N/A, not assessed.

significant safety concern. Critically, predominant astroglial cell fate after transplantation of rodent neural stem cells into animal models of SCI has been shown to correlate with both changes in CGRP sensory fiber sprouting and allodynia/hyperalgesia [23, 42–45].

Accordingly, we determined whether hCNS-SCns or the timing of transplantation following SCI altered ascending sensory fiber sprouting by performing unbiased stereological quantification of CGRP fiber volume and length in the spinal cord dorsal horn laminae III–IV in all four cohorts of SCI rats: 9 DPI vehicle; 9 DPI hCNS-SCns; 60 DPI vehicle; and 60 DPI hCNS-SCns. No significant differences were observed between any of the cohorts (Fig. 4, Student's *t* test, $p > .1$). In addition, no significant correlative relationship in the 9 DPI or 60 DPI transplant cohorts was observed between (a) CGRP volume and total SC121$^+$ human cell number, (b) CGRP volume and SC123$^+$ human astrocyte proportion, (c) CGRP fiber length and total SC121$^+$ human cell number, or (d) CGRP fiber length and SC123$^+$ human astrocyte proportion (supplemental online Table 3). These data suggest that hCNS-SCns transplantation did not induce changes in CGRP sensory fiber volume or sprouting.

Development of allodynia and hyperalgesia can be also assessed using behavioral analyses [25–29]. Critically, although ATN rats lack mature T cells, which do play a role in allodynia development [46–48], previous studies have shown that these animals can be used as a neurological pain syndrome model [46, 49]. To investigate whether hCNS-SCns induced changes in the behavioral measures of mechanical allodynia or thermal hyperalgesia in ATN rats, we assessed these parameters in all four cohorts prior to injury and 2, 7, 11, and 14 WPT.

No significant two-way interaction effects were observed between the hCNS-SCns versus the vehicle groups in the number of forepaw or hindpaw withdrawals in any of the cohorts in von Frey testing (Fig. 5A; repeated-measures two-way ANOVA, Bonferroni post hoc test, $p > .05$). Similarly, no significant two-way interaction effects in forepaw or hindpaw withdrawal time were found in Hargreaves testing (Fig. 5B; repeated-measures two-way ANOVA, Bonferroni post hoc *t* test, $p > .05$). von Frey and Hargreaves testing data from the 9 DPI cohort has been previously published (data not shown) [7]. These data suggest that hCNS-SCns transplantation did not alter CGRP fiber sprouting or contribute to the development of allodynia or hyperalgesia.

In parallel, we assessed allodynia using CatWalk kinematic analysis measures that have been shown to correlate with von Frey nociception data [28, 29]. No significant differences were observed in either hindpaw maximum intensity or duty factor between the vehicle and hCNS-SCns transplantation groups for either the 9 or 60 DPI cohort (Fig. 5C, 5D; Student's *t* test; $p > .05$). Furthermore, no significant correlations were found between allodynia or hyperalgesia measures and (a) total SC121$^+$ human cell number, (b) CGRP fiber volume, or (c) CGRP length (supplemental online Tables 3, 4). Finally, because previous studies have reported a relationship between the differentiation of transplanted cell populations along an astroglial lineage and the observation of pain syndromes, we evaluated the correlative relationship between these variables. Analysis of the change in number (von Frey) or latency (Hargreaves) of paw withdrawals normalized to preinjury baseline testing did not show any evidence to support the postinjury or post-transplantation development of allodynia or hyperalgesia (Fig. 5; supplemental online Fig. 4); specifically, paw withdrawals at all postinjury time points remained below the preinjury baseline. However, Pearson correlation coefficient analysis revealed a positive correlation between the total proportion of SC123$^+$ astrocytes and number of forepaw withdrawals in von Frey testing in the 60 DPI hCNS-SCns cohort (Fig. 6; supplemental online Table 4; Pearson $r = 0.8$; two-tailed *t* test; $p < .02$). Otherwise, no significant correlations were found between either von Frey allodynia or Hargreaves hyperalgesia measures and the total proportion of SC123$^+$ human astrocytes in either the 9 or 60 DPI transplant cohorts (Fig. 6). Altogether, regardless of the positive relationship between the total proportion of human astrocytes and the number of von Frey forepaw withdrawals in the 60 DPI transplant cohort, these data suggest that hCNS-SCns transplantation did not lead to development of allodynia or hyperalgesia in the ATN rat spinal cord injury model.

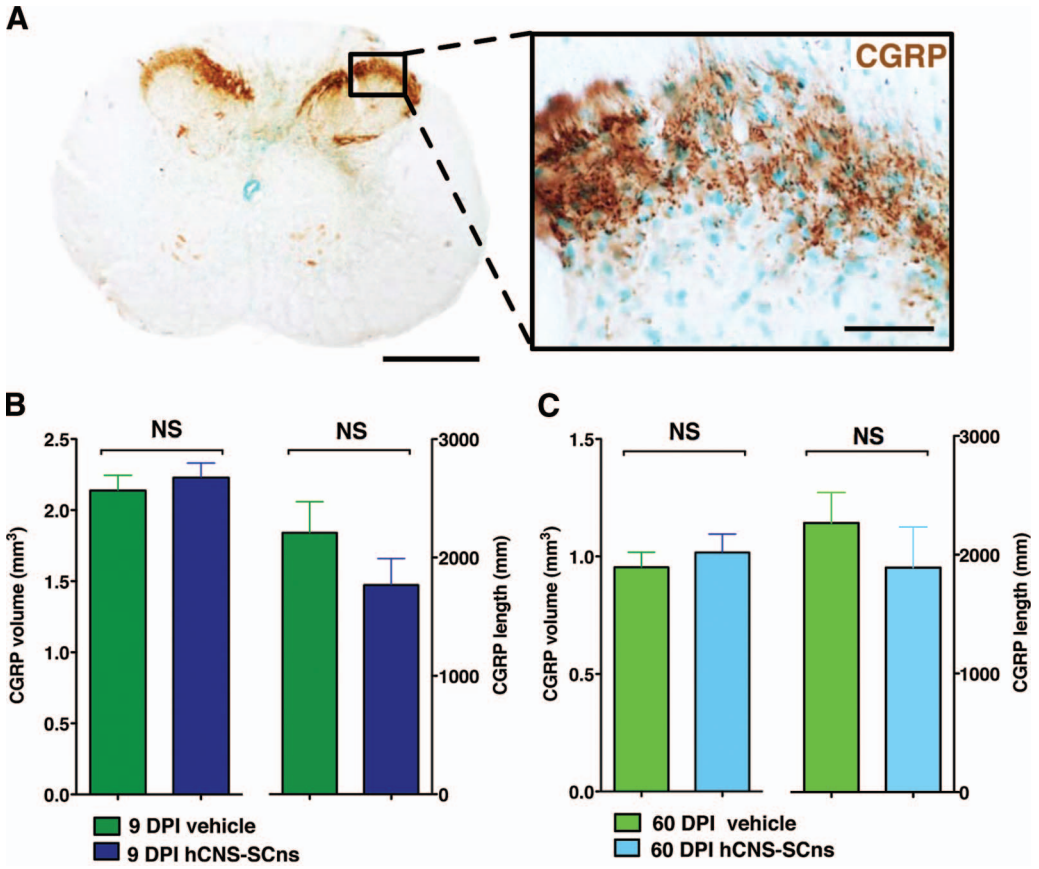

Figure 4. hCNS-SCns transplantation at 9 or 60 DPI does not alter CGRP fiber volume or sprouting in dorsal horn laminae III–IV. An example of coronal spinal cord section after immunohistochemistry using CGRP-specific antibody is shown **(A)**. Scale bars = 500 μm (left) and 50 μm (right). CGRP fiber volume and length are shown in the 9 DPI vehicle and transplant groups **(B)** and the 60 DPI vehicle and transplant groups **(C)**. No significant differences were found between the groups (Student's *t* test; $p > .5$). Error bars indicate SEM. Data were previously published in [7]. Abbreviations: CGRP, calcitonin gene-related peptide; DPI, days postinjury; hCNS-SCns, human central nervous system-derived neural stem cell; NS, not significant.

Evaluation of Locomotor Function in hCNS-SCns Transplanted Animals 14 WPT

This study focused on evaluation of the safety of hCNS-SCns in the chronic SCI microenvironment in the ATN rat. As such, the study was not designed for standard collection of multiple locomotor parameters at multiple time points of assessment. Additionally, as described in Materials and Methods, analysis of post-transplantation BBB open-field testing in ATN rats could only be completed at 14 WPT when coordination normalization data were available from the CatWalk RI parameter. Analysis of BBB locomotor scores showed no significant difference between the vehicle and the transplant cohorts at 14 WPT (Fig. 7A, 7B; Student's *t* test, $p > .05$). However, CatWalk gait analysis conducted at 14 WPT as a component of sensory behavioral assessment (as shown in Fig. 5) provided a supplemental and more sensitive measure of hind limb function. One parameter that has been used to assess locomotor recovery is hind limb base of support (BOS). BOS has been shown to increase following SCI to compensate for impaired gait and decrease as locomotor recovery improves [31, 50, 51]. No significant difference was found in hind limb BOS between the 9 DPI transplant and vehicle cohort (Fig. 7C; Student's two-tailed *t* test; $p > .05$), suggesting that hCNS-SCns transplantation in the subacute stage of SCI neither impaired nor improved locomotor recovery in ATN rats. However, a significant decrease in hind limb BOS was found between the 60 DPI hCNS-SCns and the 60 DPI vehicle cohort (Fig. 7D; Student's two-tailed *t* test; $p < .04$). No other significant differences in CatWalk parameters were observed. These data suggest, although at a single time point measurement, that hCNS-SCns transplantation into the more chronic SCI microenvironment may have improved locomotor function in ATN rats with thoracic SCI.

Discussion

The goal of this study was to investigate the safety of hCNS-SCns in the chronic SCI microenvironment in the ATN rat, comparing parenchymal transplantation at either 9 or 60 DPI, and assessing human cell engraftment (survival), migration, fate, and development of anatomical or behavioral evidence of neurological pain. Previous preclinical transplantation studies evaluating the effect of rodent neural stem cells or human embryonic stem cell-derived oligodendrocyte progenitors in the chronic SCI microenvironment at 2 months or more postinjury have shown either unsuccessful or low engraftment [52–54]. Accordingly, direct comparison of subacute and chronic transplantation times in a single study is an important step in evaluating overall engraftment as well as the interaction of transplanted cells within the host microenvironment (e.g., in the context of fate potential). In addition, quantification of human cell engraftment and safety

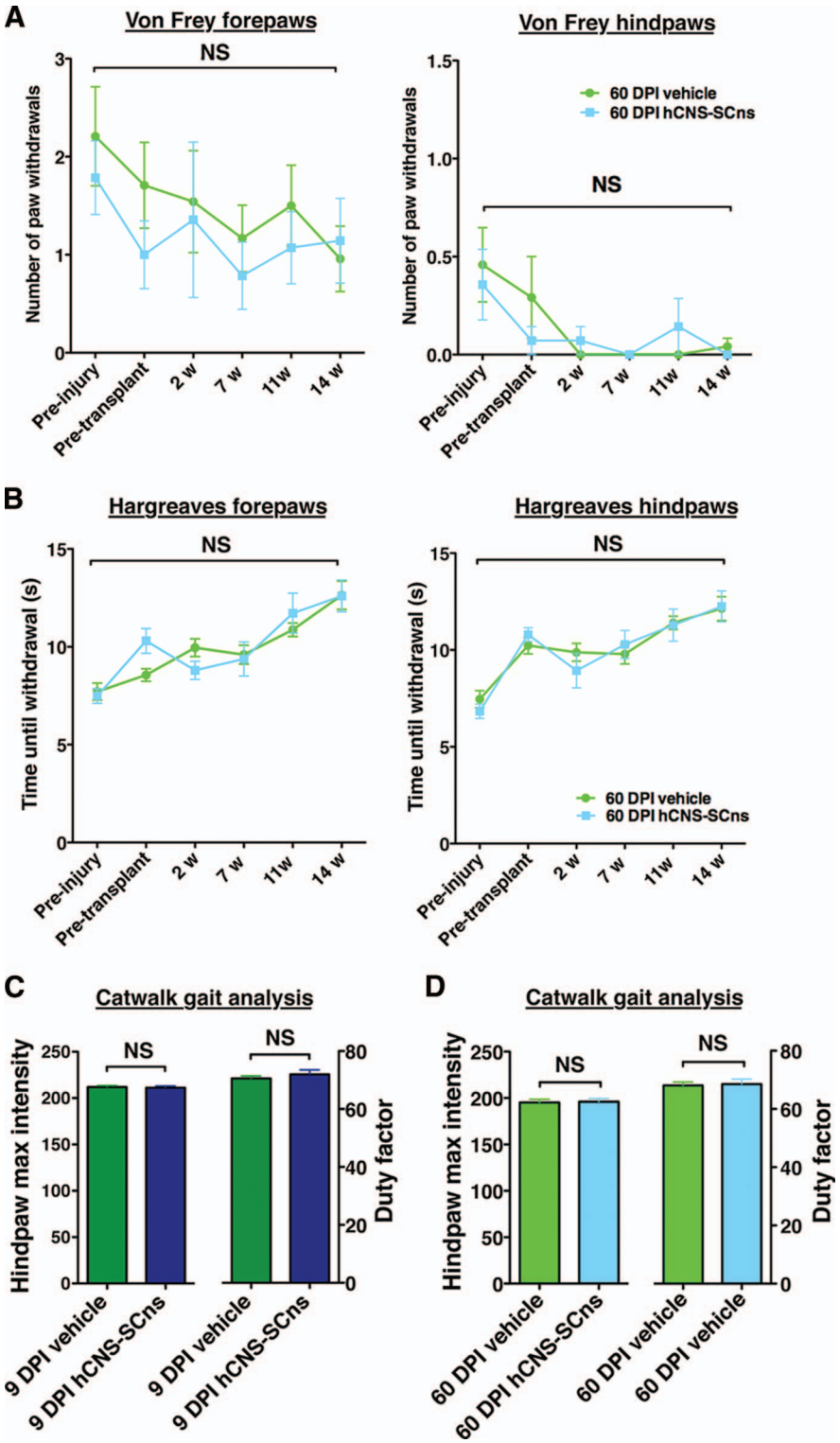

Figure 5. hCNS-SCns transplantation at 9 or 60 DPI does not contribute to development of allodynia or hyperalgesia. Analyses were conducted by repeated-measures two-way analysis of variance (ANOVA). von Frey allodynia testing **(A)** revealed that no significant two-way interaction effects were found between the number of forepaw and hindpaw withdrawals in the 60 DPI hCNS-SCns cohort over time (black brackets), and no significant differences were observed between the vehicle and the transplant group at any time point of analysis (preinjury or 2, 7, 11, or 14 weeks post-transplantation [WPT]; Bonferroni post hoc test, $p > .05$). No significant two-way interaction effects were found in Hargreaves hyperalgesia testing **(B)** between forepaw and hindpaw withdrawal time in the 60 DPI hCNS-SCns cohort over time (black brackets), and no significant differences were observed between the vehicle and the transplant group at any time point of analysis (preinjury or 2, 7, 11, or 14 WPT; Bonferroni post hoc test, $p > .05$). At 14 WPT, CatWalk gait analysis revealed no significant differences in hindpaw maximum intensity (one-way ANOVA; $p > .05$) or in the duty factor (one-way ANOVA; $p > .05$) between the vehicle and the hCNS-SCns cohorts transplanted at 9 DPI **(C)** or 60 DPI **(D)**. Error bars indicate SEM. Abbreviations: DPI, days postinjury; hCNS-SCns, human central nervous system-derived neural stem cell; NS, not significant; w, weeks.

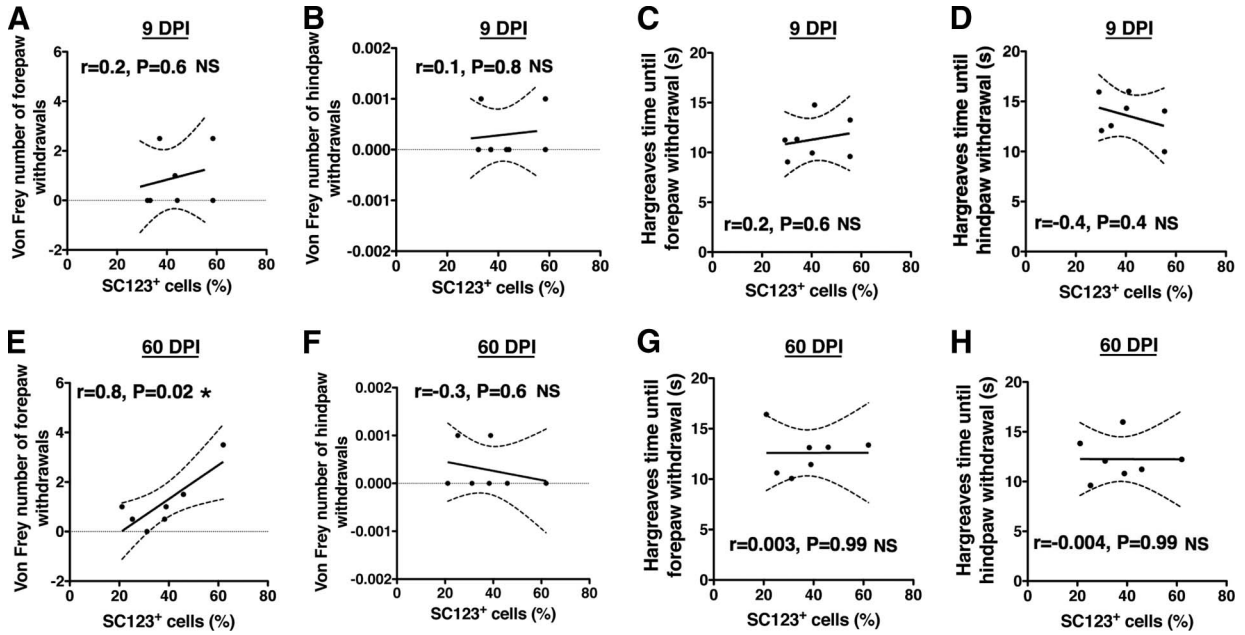

Figure 6. Correlations between von Frey and Hargreaves sensory behavior testing and the total proportion of human SC123$^+$ astrocytes in the 9 DPI and 60 DPI transplant cohorts at 14 weeks post-transplantation (WPT). No relationship was found between the proportion of human SC123$^+$ astrocytes in the 9 DPI human central nervous system-derived neural stem cell (hCNS-SCns) cohort and either the number of forepaw **(A)** and hindpaw **(B)** withdrawals in von Frey testing, or the time until forepaw **(C)** and hindpaw **(D)** withdrawal in Hargreaves testing at 14 WPT (Pearson $r = 0.2$, two-tailed t test; $p > .6$; $r = 0.1$, $p > .8$; $r = 0.2$, $p > .6$; and $r = -0.4$, $p > .4$, respectively). Although no histological or sensory behavioral evidence of development of neurological pain syndromes was found in any of the hCNS-SCns transplant cohorts, a positive correlation was found between the number of forepaw withdrawals in von Frey testing and the proportion of human SC123$^+$ astrocytes **(E)** in the 60 DPI hCNS-SCns cohort at 14 WPT (Pearson $r = 0.8$, $p < .02$). No relationship was found between the proportion of human SC123$^+$ astrocytes in the 60 DPI hCNS-SCns cohort and either the number of hindpaw withdrawals **(F)** in von Frey, or the time until forepaw **(G)** or hindpaw **(H)** withdrawal in Hargreaves at 14 WPT (Pearson $r = -0.3$, $p > .6$; $r = 0.003$, $p > .99$; and $r = -0.004$, $p > .99$, respectively). *xy* scatter plots show individual data points (dots) and curve fit with $\pm$SEM (dashed lines). If all animals in a cohort exhibited a sensory behavioral value of 0 (gray line), for statistical analysis the values of two randomly selected animals were labeled as 0.001. Abbreviations: DPI, days postinjury; NS, not significant.

parameters in a rat versus mouse SCI model provides insight into the effect of cell transplantation into a local microenvironment in which a fluid filled cystic cavity is evolving over time, similar to the development of a syrinx in the human clinical setting.

One factor contributing to engraftment success is the presence of cell lineage-specific survival, growth, and/or differentiation cues [55–59]. In this regard, the CNS injury microenvironment is dynamic; in particular, the composition and concentration of inflammation-related cells and molecules [11, 20, 60, 61] (Hooshmand MJ, Nguyen HX, Hong S et al., submitted for publication), as well as endogenous growth factors [62, 63], change dramatically between acute and chronic SCI. These aspects of the microenvironment are paralleled by similarly dynamic changes in both lesion and spared tissue volume over time [35]. Furthermore, there is evidence of host repair during the postinjury period, including spontaneous remyelination, which may alter the functional targets for cell integration [64–67]. This suggests that transplanted cells will encounter not only a different microenvironment but also a different number of potential targets for integration in different post-SCI periods.

It is well-established that chemical and material properties contribute to defining the stem cell niche in vitro [68] and that niche size is tightly regulated for hematopoietic and other stem cell populations in vivo [69, 70]. Accordingly, in addition to postinjury transplantation timing, the potential contribution of injury magnitude and location in defining the size of the niche into which donor cells can integrate, and the number of targets available for donor cell integration, should be considered as important variables for cell engraftment and efficacy. Conversely, the interaction of niche size with cell dose is also likely to be an important factor. Critically, the total number of engrafted donor cells alone will not necessarily define repair. Rather, the combination of cell engraftment, cell fate, and cell migration within the host niche may be critical. Toward this point, we report here that the time of transplantation after injury influenced both the capacity for generation of mature oligodendrocytes and the potential for functional locomotor recovery.

Unlike constitutively immunodeficient animal models, immunocompetent or immunosuppressed transplant models do not permit the evaluation of xenogeneic donor cell expansion after transplantation [55]. We have previously reported that both subacute and delayed 30 DPI hCNS-SCns transplantation in the NOD-scid mouse SCI model results in an approximately threefold increase in total human cell number over the initial cell transplant dose [4–6]. In accordance with our previous data, immunodeficient ATN rats in the chronic 60 DPI transplant cohort exhibited good engraftment and 2.5-fold increase in total human cell number over the initial cell transplant dose by 14 WPT. However, the total cell numbers in this cohort remained lower when compared with the subacute 9 DPI transplant cohort, which exhibited a fivefold increase in total human cell number over the initial cell transplant dose. Overall, the magnitude of donor cell expansion in the 9 DPI ATN SCI model was increased when compared with our previous observations in constitutively

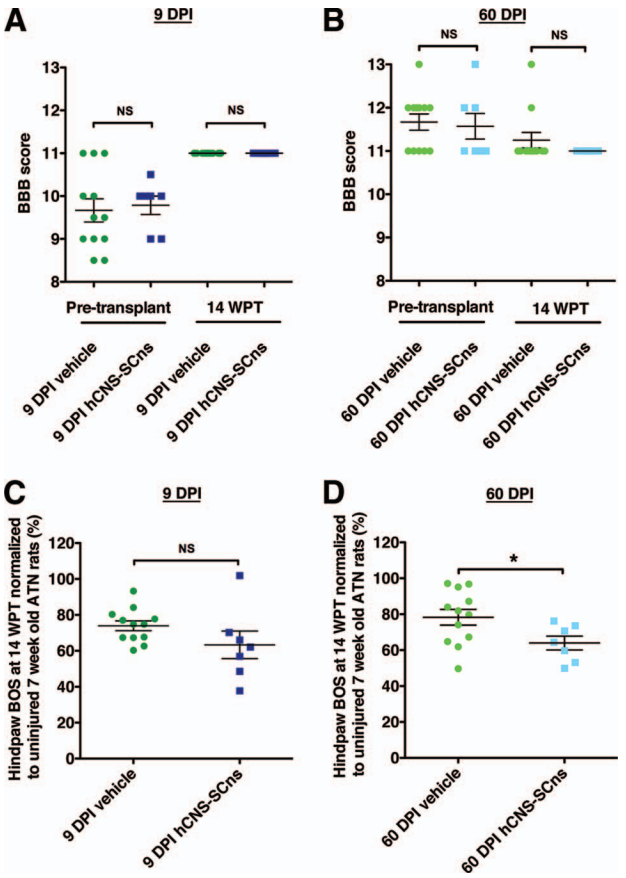

Figure 7. hCNS-SCns transplanted ATN rats exhibit no evidence of a decline in locomotor function at 14 WPT. Pretransplant or 14 WPT BBB locomotor scores showed no significant difference between the 9 DPI vehicle and the 9 DPI transplant cohorts **(A)**, or the 60 DPI vehicle and the 60 DPI transplant cohorts **(B)**, suggesting that hCNS-SCns did not cause a decline in locomotor function at 14 WPT. BBB scores at 14 WPT were corrected to CatWalk regularity index at 14 WPT. CatWalk gait measure of hind limb BOS **(C)** normalized to a baseline obtained in uninjured ATN rats assessed at 7 weeks of age revealed no difference between the 9 DPI vehicle and the 9 DPI hCNS-SCns cohorts at 14 WPT (Student's *t* test; $p > .05$). However, animals in the 60 DPI hCNS-SCns cohort exhibited significantly decreased normalized hind limb BOS compared with that in the vehicle 60 DPI cohort at 14 WPT (Student's *t* test; $*$, $p < .04$) **(D)**, suggesting that hCNS-SCns transplantation at 60 DPI may have a potential to improve locomotor recovery at 14 WPT. Error bars indicate SEM. Abbreviations: ATN, athymic nude; BBB, Basso, Beattie, and Bresnahan; BOS, base of support; DPI, days postinjury; hCNS-SCns, human central nervous system-derived neural stem cell; NS, not significant; WPT, weeks post-transplantation.

immunodeficient mice. Importantly, however, this was paralleled by an increase in the incidence of graft failure, with a total of 30% of transplanted animals in the combined 9 and 60 DPI cohorts failing to exhibit human cell engraftment at the end of the study. In contrast, we have not previously observed graft failure in NOD-scid or Rag2γ mice. This difference is likely to result from the well-characterized compensatory increase in natural killer cell number in the ATN strain [7, 55].

Although donor cells clearly show the capacity for expansion in the SCI microenvironment, we have found that proliferation is predominantly restricted to the first few weeks after transplantation (Sontag CJ, Uchida N, Cummings BJ et al., submitted for publication; Piltti KM, Avakian SN, Funes GM et al., manuscript in preparation). In fact, nearly all hCNS-SCns have arrested their cell cycle by 14–16 WPT, and only 1%–3% of human cells exhibited mitotic markers at 16 WPT (Piltti KM, Avakian SN, Funes GM et al., manuscript in preparation). These data are in accordance with the current study, which showed that 97%–99% of human cells expressed lineage-specific markers at 14 WPT. In addition, no evidence of abnormal cellular morphology, mass formation, or tumorigenesis was observed in any of these studies.

The development of neurological pain has previously been reported in animals receiving transplants of genetically modified or immortalized murine neural stem cells after SCI [23, 72]; this observation was associated with predominant astrogliogenesis and alterations in sprouting of CGRP sensory fibers. Contrary to these reports, and in accordance with our previous transplantation studies with hCNS-SCns [6, 7], no histological or sensory behavioral evidence of development of neurological pain syndromes was found in any of the cohorts at 14 WPT. Although a greater proportion of donor cells evidenced an astroglial phenotypic fate after transplantation into the ATN rat model used here in comparison with our previous studies in immunodeficient mouse models, this population was still less than the combined oligodendroglial and neuronal population. We did find a positive correlation between the total proportion of human astrocytes and the number of von Frey forepaw withdrawals in the 60 DPI animals; however, the change in paw sensitivity remained below the preinjury level. Interestingly, astrocytes have recently been shown to participate in the normal physiological response to sensory stimulation in the spinal cord [73], as well as in synaptic remodeling after CNS injury [74]. Furthermore, consistent with our observation of sensory function modulation in the absence of allodynia or hyperalgesia, transplantation of derived astrocytes has recently been suggested to improve sensory recovery after SCI [75]. Further evaluation of the relationship between phenotypic and functional astrocytic cell fate and sensory outcome may yield insight into the complex roles of these cells in the CNS.

The proportion of human GFAP- and DCX-positive hCNS-SCns was unaltered in the 60 DPI compared with 9 DPI transplant cohorts. Similarly, in agreement with our previously reported data in NOD-scid mice [4–7], the majority of transplanted hCNS-SCns differentiated into oligodendrocytic lineage cells (>50%). However, the chronic 60 DPI transplantation cohort exhibited a proportion of human oligodendroglial cells (14%) positive only for CC-1, suggesting that the proportion of mature oligodendrocytes was increased. Although the role of chronic demyelination in the locomotor deficits associated with SCI is controversial, restoration of axonal conduction by cellular remyelination has been one strategy to restore function [4, 64, 76–82]. Although there is clearly spontaneous remyelination after SCI [65, 67, 83–86], persistent demyelination has been reported chronically postinjury in animals and humans [77, 87–91]. In this regard, it is interesting that although the animals in 60 DPI transplant cohort had fewer human cells, the data suggest that the proportion of mature human oligodendrocytes was increased in these animals.

We have previously reported functional recovery following early chronic (30 DPI) [6] and subacute (9 DPI) hCNS-SCns transplantation in immunodeficient NOD-scid mice [4, 5], as well as in chronic (60 DPI) transplantation immunosuppressed C57BL/6 mice [92]. This study focused on evaluation of allodynia and hyperalgesia in an SCI model that exhibits cavitation. However, 14

WPT CatWalk gait analysis conducted as a component of sensory behavioral assessment yielded insight into locomotor performance, demonstrating a significant reduction in BOS in the 60 DPI transplant cohort animals and suggesting that hCNS-SCns transplantation in chronic SCI may have improved locomotor recovery. No significant difference was found in CatWalk BOS or BBB scores between the 9 DPI vehicle and 9 DPI hCNS-SCns cohort, suggesting cell transplantation at this time neither impaired nor improved function. Lack of detection of functional recovery in the 9 DPI transplantation cohort in the current study could reflect several factors. First, as we describe, assessment of locomotion in the ATN rat strain is difficult in comparison with other rodents. Second, as noted, this study was not designed for standard collection of multiple locomotor parameters at multiple time points of assessment. Third, this study included a relatively small number of animals in the transplant cohorts ($n = 7$), impairing statistical power for locomotor metrics [13, 93]. Finally, integration of a sufficient proportion of mature human oligodendrocytes could be linked to the potential for functional locomotor recovery.

Conclusion

Taken together, these data suggest that hCNS-SCns transplantation in either the subacute or chronic SCI microenvironment of immunodeficient rats produced a pattern of cell engraftment, migration, and differentiation that is consistent with previous results in immunodeficient mice. hCNS-SCns transplantation did not result in anatomical or behavioral evidence of neurological pain, and no evidence for adverse effects was observed in any transplantation cohort.

Acknowledgments

We thank the Christopher and Dana Reeve Foundation SCI Core Facility, especially Rebecca Nishi and Hongli-Liu for their help with animal surgeries. We also thank Kevin Beck, Colleen Worne, Ara Salibian, Kameelah Abdullah, Daniel Cantu, Kevin Huang, and Antoinette Hu for technical assistance. This work was supported by National Institutes of Health/National Institute of Neurological Disorders and Stroke (Grant R01-NS049885) and the Christopher Reeve Foundation (AAC-2005) to A.J.A.; by California Institute for Regenerative Medicine (CIRM) Stem Cell Training Grant T1-00008 and the University of California's Alliance for Graduate Education and the Professoriate (UC AGEP) Fellowship National Science Foundation (NSF) HRD0450366 to D.L.S.; and by CIRM Postdoctoral Training Grant TG2-01152 to K.M.P.

Author Contributions

K.M.P.: collection and/or assembly of data, data analysis and interpretation, manuscript writing; D.L.S.: collection and/or assembly of data, data analysis and interpretation; N.U.: provision of study material, data analysis and interpretation; B.J.C.: conception and design, data analysis and interpretation, manuscript writing; A.J.A.: conception and design, financial support, data analysis and interpretation, manuscript writing, final approval of manuscript.

Disclosure of Potential Conflicts of Interest

N.U. is a compensated employee of StemCells Inc. B.J.C. has compensated research funding and an uncompensated, unrestricted research gift.

References

1 Wyndaele M, Wyndaele JJ. Incidence, prevalence and epidemiology of spinal cord injury: What learns a worldwide literature survey? Spinal Cord 2006;44:523–529.

2 van den Berg M, Castellote J, Mahillo-Fernandez I et al. Incidence of spinal cord injury worldwide: A systematic review. Neuroepidemiology;34:184.

3 Devivo M. Epidemiology of traumatic spinal cord injury: Trends and future implications. Spinal Cord 2012;50:365–372.

4 Cummings BJ, Uchida N, Tamaki SJ et al. Human neural stem cells differentiate and promote locomotor recovery in spinal cord-injured mice. Proc Natl Acad Sci USA 2005;102: 14069–14074.

5 Hooshmand MJ, Sontag CJ, Uchida N et al. Analysis of host-mediated repair mechanisms after human CNS-stem cell transplantation for spinal cord injury: Correlation of engraftment with recovery. PLoS One 2009;4:e5871.

6 Salazar DL, Uchida N, Hamers FP et al. Human neural stem cells differentiate and promote locomotor recovery in an early chronic spinal cord injury NOD-scid mouse model. PLoS One 2010;5:e12272.

7 Piltti KM, Salazar DL, Uchida N et al. Safety of epicenter versus intact parenchyma as a transplantation site for human neural stem cells for spinal cord injury therapy. Stem Cells Translational Medicine 2013;2:204–216.

8 Tetzlaff W, Okon E, Karimi-Abdolrezaee S et al. A systematic review of cellular transplantation therapies for spinal cord injury. J Neurotrauma 2011;28:1611–1682.

9 Fawcett J, Curt A, Steeves J et al. Guidelines for the conduct of clinical trials for spinal cord injury as developed by the ICCP panel: Spontaneous recovery after spinal cord injury and statistical power needed for therapeutic clinical trials. Spinal Cord 2007;45:190–205.

10 Srinivas TR, Meier-Kriesche H-U. Minimizing immunosuppression, an alternative approach to reducing side effects: Objectives and interim result. Clin J Am Soc Nephrol 2008; 3(suppl 2):S101–S116.

11 Cummings BJ, Hooshmand MJ, Salazar DL et al. Human neural stem cell mediated repair of the contused spinal cord: Timing the microenvironment. In: Ribak CE, Arámburo de la Hoz C, Jones EG et al., eds. From Development to Degeneration and Regeneration of the Nervous System. Oxford, U.K.: Oxford University Press, 2009:297–322.

12 Houle J, Tessler A. Repair of chronic spinal cord injury. Exp Neurol 2003;182:247–260.

13 Basso D, Beattie M, Bresnahan J. A sensitive and reliable locomotor rating scale for open field testing in rats. J Neurotrauma 1995; 12:1–21.

14 Hill C, Beattie M, Bresnahan J. Degeneration and sprouting of identified descending supraspinal axons after contusive spinal cord injury in the rat. Exp Neurol 2001;171:153–169.

15 Anderson A. Mechanisms and pathways of inflammatory responses in CNS trauma: Spinal cord injury. J Spinal Cord Med 2002;25:70.

16 Jones T, McDaniel E, Popovich P. Inflammatory-mediated injury and repair in the traumatically injured spinal cord. Curr Pharm Des 2005;11:1223–1236.

17 Popovich P, Jones T. Manipulating neuroinflammatory reactions in the injured spinal cord: Back to basics. Trends Pharmacol Sci 2003;24:13–17.

18 Schwartz M, Butovsky O, Brück, W et al. Microglial phenotype: Is the commitment reversible? Trends Neurosci 2006;29:68–74.

19 Kigerl K, McGaughy V, Popovich P. Comparative analysis of lesion development and intraspinal inflammation in four strains of mice following spinal contusion injury. J Comp Neurol 2006;494:578–594.

20 Beck KD, Nguyen HX, Galvan MD et al. Quantitative analysis of cellular inflammation after traumatic spinal cord injury: Evidence for a multiphasic inflammatory response in the acute to chronic environment. Brain 2010;133: 433–447.

21 Chow S, Moul J, Tobias C et al. Characterization and intraspinal grafting of EGF/bFGF-dependent neurospheres derived from embryonic rat spinal cord. Brain Res 2000;874: 87–193.

22 Cao Q, Zhang Y, Howard R et al. Pluripotent stem cells engrafted into the normal or lesioned adult rat spinal cord are restricted to a glial lineage. Exp Neurol 2001;167:48–106.

23 Macias M, Syring M, Pizzi M et al. Pain with no gain: Allodynia following neural stem cell transplantation in spinal cord injury. Exp Neurol 2006;201:335–383.

24 Kumamaru H, Kobayakawa K, Saiwai H et al. The therapeutic activities of engrafted neural stem/precursor cells are not dormant in the chronically injured spinal cord. STEM CELLS 2013; 31:1535–1547.

25 Hargreaves K, Dubner R, Brown F et al. A new and sensitive method for measuring thermal nociception in cutaneous hyperalgesia. Pain 1988;32:77–165.

26 Hains B, Johnson K, Eaton M et al. Serotonergic neural precursor cell grafts attenuate bilateral hyperexcitability of dorsal horn neurons after spinal hemisection in rat. Neuroscience 2003;116:1097–1207.

27 Horiuchi H, Ogata T, Morino T et al. Adenosine A1 receptor agonists reduce hyperalgesia after spinal cord injury in rats. Spinal Cord 2010;48:685–690.

28 Gabriel A, Marcus M, Honig WM et al. The CatWalk method: A detailed analysis of behavioral changes after acute inflammatory pain in the rat. J Neurosci Methods 2007;163: 9–25.

29 Vrinten D, Hamers F. "CatWalk" automated quantitative gait analysis as a novel method to assess mechanical allodynia in the rat: A comparison with von Frey testing. Pain 2003;102:203–212.

30 Uchida N, Buck DW, He D et al. Direct isolation of human central nervous system stem cells. Proc Natl Acad Sci USA 2000;97: 14720–14725.

31 Hamers F, Koopmans G, Joosten E. CatWalk-assisted gait analysis in the assessment of spinal cord injury. J Neurotrauma 2006;23: 537–548.

32 Muja N, Cohen M, Zhang J et al. Neural precursors exhibit distinctly different patterns of cell migration upon transplantation during either the acute or chronic phase of EAE: A serial MR imaging study. Magn Reson Med. 2011; 65:1738–1749.

33 Potas J, Zheng Y, Moussa C et al. Augmented locomotor recovery after spinal cord injury in the athymic nude rat. J Neurotrauma 2006;23:660–673.

34 Gorrie C, Hayward I, Cameron N et al. Effects of human OEC-derived cell transplants in rodent spinal cord contusion injury. Brain Res 2010;1337:8–20.

35 Rabchevsky A, Fugaccia I, Sullivan P et al. Efficacy of methylprednisolone therapy for the injured rat spinal cord. J Neurosci Res 2002;68: 7–18.

36 Sugimori M, Nagao M, Parras C et al. Ascl1 is required for oligodendrocyte development in the spinal cord. Development 2008; 135:1271–1281.

37 Zhu X, Zuo H, Maher B et al. Olig2-dependent developmental fate switch of NG2 cells. Development 2012;139:2299–2307.

38 Carlton S, McNeill D, Chung K et al. A light and electron microscopic level analysis of calcitonin gene-related peptide (CGRP) in the spinal cord of the primate: An immunohistochemical study. Neurosci Lett 1987;82:145–150.

39 Ackery A, Norenberg M, Krassioukov A. Calcitonin gene-related peptide immunoreactivity in chronic human spinal cord injury. Spinal Cord 2007;45:678–686.

40 Ondarza A, Ye Z, Hulsebosch C. Direct evidence of primary afferent sprouting in distant segments following spinal cord injury in the rat: Colocalization of GAP-43 and CGRP. Exp Neurol 2003;184:373–380.

41 Finnerup N. Pain in patients with spinal cord injury. Pain 2012, 10.1016/j.pain.2012. 12.007.

42 Davies J, Pröschel C, Zhang N et al. Transplanted astrocytes derived from BMP- or CNTF-treated glial-restricted precursors have opposite effects on recovery and allodynia after spinal cord injury. J Biol 2008;7:24.

43 Hofstetter C, Schwarz E, Hess D et al. Marrow stromal cells form guiding strands in the injured spinal cord and promote recovery. Proc Natl Acad Sci USA 2002;99:2199–2403.

44 Calmels P, Mick G, Perrouin-Verbe B et al. Neuropathic pain in spinal cord injury: Identification, classification, evaluation. Ann Phys Rehabil Med 2009;52:83–185.

45 Christensen M, Hulsebosch C. Chronic central pain after spinal cord injury. J Neurotrauma 1997;14:517–537.

46 Moalem G, Xu K, Yu L. T lymphocytes play a role in neuropathic pain following peripheral nerve injury in rats. Neuroscience 2004;129: 767–777.

47 Cao L, DeLeo J. CNS-infiltrating CD4+ T lymphocytes contribute to murine spinal nerve transection-induced neuropathic pain. Eur J Immunol 2008;38:448–458.

48 Costigan M, Moss A, Latremoliere A et al. T-cell infiltration and signaling in the adult dorsal spinal cord is a major contributor to neuropathic pain-like hypersensitivity. J Neurosci 2009;29:14415–14422.

49 Liu H, Shiryaev S, Chernov A et al. Immunodominant fragments of myelin basic protein initiate T cell-dependent pain. J Neuroinflamm 2012;9:119.

50 Hamers F, Lankhorst A, van Laar T et al. Automated quantitative gait analysis during overground locomotion in the rat: Its application to spinal cord contusion and transection injuries. J Neurotrauma 2001;18:187–201.

51 Eaton M, Pearse D, McBroom J et al. The combination of human neuronal serotonergic cell implants and environmental enrichment after contusive SCI improves motor recovery over each individual strategy. Behav Brain Res 2008;194:236–241.

52 Karimi-Abdolrezaee S, Eftekharpour E, Wang J et al. Delayed transplantation of adult neural precursor cells promotes remyelination and functional neurological recovery after spinal cord injury. J Neurosci 2006;26:3377–3389.

53 Keirstead HS, Nistor G, Bernal G et al. Human embryonic stem cell-derived oligodendrocyte progenitor cell transplants remyelinate and restore locomotion after spinal cord injury. J Neurosci 2005;25:4694–4705.

54 Pfeifer K, Vroemen M, Caioni M et al. Autologous adult rodent neural progenitor cell transplantation represents a feasible strategy to promote structural repair in the chronically injured spinal cord. Regen Med 2006;1:255–266.

55 Anderson A, Haus D, Hooshmand M et al. Achieving stable human stem cell engraftment and survival in the CNS: Is the future of regenerative medicine immunodeficient? Regen Med 2011;6:367–773.

56 Martino G, Pluchino S, Bonfanti L et al. Brain regeneration in physiology and pathology: The immune signature driving therapeutic plasticity of neural stem cells. Physiol Rev 2011;91:1281–1304.

57 Kokaia Z, Martino G, Schwartz M et al. Cross-talk between neural stem cells and immune cells: The key to better brain repair? Nat Neurosci 2012;15:1078–1087.

58 Sharma M, Afrin F, Satija N et al. Stromal-derived factor-1/CXCR4 signaling: Indispensable role in homing and engraftment of hematopoietic stem cells in bone marrow. Stem Cells Dev 2011;20:933–946.

59 Bouchentouf M, Benabdallah B, Bigey P et al. Vascular endothelial growth factor reduced hypoxia-induced death of human myoblasts and improved their engraftment in mouse muscles. Gene Ther 2008;15:404–414.

60 Anderson AJ, Robert S, Huang W et al. Activation of complement pathways after contusion-induced spinal cord injury. J Neurotrauma 2004;21:1831–1846.

61 Monje M, Toda H, Palmer T. Inflammatory blockade restores adult hippocampal neurogenesis. Science 2003;302:1760–1765.

62 Mocchetti I, Wrathall J. Neurotrophic factors in central nervous system trauma. J Neurotrauma 1995;12:853–870.

63 Bareyre F, Schwab M. Inflammation, degeneration and regeneration in the injured spinal cord: Insights from DNA microarrays. Trends Neurosci 2003;26:555–563.

64 Blight A, Young W. Central axons in injured cat spinal cord recover electrophysiological function following remyelination by Schwann cells. J Neurol Sci 1989;91:15–34.

65 Powers B, Lasiene J, Plemel J et al. Axonal thinning and extensive remyelination without chronic demyelination in spinal injured rats. J Neurosci 2012;32:5120–5125.

66 Powers B, Sellers D, Lovelett E et al. Remyelination reporter reveals prolonged refinement of spontaneously regenerated myelin. Proc Natl Acad Sci USA 2013;110:4075–4080.

67 Lasiene J, Shupe L, Perlmutter S et al. No evidence for chronic demyelination in spared axons after spinal cord injury in a mouse. J Neurosci 2008;28:3887–3896.

68 Jiang J, Papoutsakis E. Stem-cell niche based comparative analysis of chemical and nano-mechanical material properties impacting ex vivo expansion and differentiation of hematopoietic and mesenchymal stem cells. Adv Healthc Mater 2013;2:25–42.

69 Voog J, Jones D. Stem cells and the niche: A dynamic duo. Cell Stem Cell 2010;6:103–115.

70 Zhang J, Niu C, Ye L et al. Identification of the haematopoietic stem cell niche and control of the niche size. Nature 2003;425:836–841.

71 Sontag CJ, Uchida N, Cummings BJ et al. The injured spinal cord niche alters the engraftment dynamics of human neural stem cells. Stem Cell Rep 2013 (in press).

72 Hofstetter C, Holmström N, Lilja J et al. Allodynia limits the usefulness of intraspinal neural stem cell grafts; directed differentiation improves outcome. Nat Neurosci 2005;8:346–399.

73 Cirillo G, De Luca D, Papa M. Calcium imaging of living astrocytes in the mouse spinal

cord following sensory stimulation. Neural Plast 2012;2012:425818.

74 Takatsuru Y, Eto K, Kaneko R et al. Critical role of the astrocyte for functional remodeling in contralateral hemisphere of somatosensory cortex after stroke. J Neurosci 2013;33:4683–4692.

75 Jin Y, Neuhuber B, Singh A et al. Transplantation of human glial restricted progenitors and derived astrocytes into a contusion model of spinal cord injury. J Neurotrauma 2011;28:579–594.

76 Eftekharpour E, Karimi-Abdolrezaee S, Fehlings M. Current status of experimental cell replacement approaches to spinal cord injury. Neurosurg Focus 2008;24:E19.

77 Guest J, Hiester E, Bunge R. Demyelination and Schwann cell responses adjacent to injury epicenter cavities following chronic human spinal cord injury. Exp Neurol 2005;192:384–393.

78 Nashmi R, Fehlings M. Changes in axonal physiology and morphology after chronic compressive injury of the rat thoracic spinal cord. Neuroscience 2001;104:235–251.

79 Nori S, Okada Y, Yasuda A et al. Grafted human-induced pluripotent stem-cell-derived neurospheres promote motor functional recovery after spinal cord injury in mice. Proc Natl Acad Sci USA 2011;108:16825–16830.

80 Tsuji O, Miura K, Okada Y et al. Therapeutic potential of appropriately evaluated safe-induced pluripotent stem cells for spinal cord injury. Proc Natl Acad Sci USA 2010;107:12704–12709.

81 Tamaki S, Jacobs Y, Dohse M et al. Neuroprotection of host cells by human central nervous system stem cells in a mouse model of infantile neuronal ceroid lipofuscinosis. Cell Stem Cell 2009;5:310–319.

82 Uchida N, Chen K, Dohse M et al. Human neural stem cells induce functional myelination in mice with severe dysmyelination. Sci Transl Med 2012;4:155ra136.

83 Gledhill R, Harrison B, McDonald W. Demyelination and remyelination after acute spinal cord compression. Exp Neurol 1973;38:472–487.

84 Harrison B, McDonald W. Remyelination after transient experimental compression of the spinal cord. Ann Neurol 1977;1:542–551.

85 Salgado-Ceballos H, Guizar-Sahagun G, Feria-Velasco A et al. Spontaneous long-term remyelination after traumatic spinal cord injury in rats. Brain Res 1998;782:126–135.

86 Smith P, Jeffery N. Histological and ultrastructural analysis of white matter damage after naturally-occurring spinal cord injury. Brain Pathol 2006;16:99–109.

87 Arvanian V, Schnell L, Lou L et al. Chronic spinal hemisection in rats induces a progressive decline in transmission in uninjured fibers to motoneurons. Exp Neurol 2009;216:471–480.

88 Baptiste D, Fehlings M. Pharmacological approaches to repair the injured spinal cord. J Neurotrauma 2006;23:318–334.

89 Bunge R, Puckett W, Becerra J et al. Observations on the pathology of human spinal cord injury. A review and classification of 22 new cases with details from a case of chronic cord compression with extensive focal demyelination. Adv Neurol 1993;59:75–89.

90 Hunanyan A, Alessi V, Patel S et al. Alterations of action potentials and the localization of Nav1.6 sodium channels in spared axons after hemisection injury of the spinal cord in adult rats. J Neurophysiol 2011;105:1033–1044.

91 Totoiu M, Keirstead H. Spinal cord injury is accompanied by chronic progressive demyelination. J Comp Neurol 2005;486:373–383.

92 Sontag CJ, Nguyen HX, Kamei N et al. Immunosuppressants affect human neural stem cells in vitro but not in an in vivo model of spinal cord injury. Stem Cells Translational Medicine 2013;2:731–744.

93 Basso D, Beattie M, Bresnahan J. Graded histological and locomotor outcomes after spinal cord contusion using the NYU weight-drop device versus transection. Exp Neurol 1996;139:244–256.

See www.StemCellsTM.com for supporting information available online.